scientific reports

Check for updates

OPEN

Identification of dequalinium as a potent inhibitor of human organic cation transporter 2 by machine learning based QSAR model

Fumihiro Yamane[1], Kenji Ikemura[2]✉, Masayoshi Kondo[1], Manami Ueno[1] & Masahiro Okuda[2]

Human organic cation transporter 2 (hOCT2/*SLC22A2*) is a key drug transporter that facilitates the transport of endogenous and exogenous organic cations. Because hOCT2 is responsible for the development of adverse effects caused by platinum-based anti-cancer agents, drugs with OCT2 inhibitory effects may serve as prophylactic agents against the toxicity of platinum-based anti-cancer agents. In the present study, we established a machine learning-based quantitative structure–activity relationship (QSAR) model for hOCT2 inhibitors based on the public ChEMBL database and explored novel hOCT2 inhibitors among the FDA-approved drugs. Using our QSAR model, we identified 162 candidate hOCT2 inhibitors among the FDA-approved drugs registered in the DrugBank database. After manual selection and in vitro assays, we found that dequalinium, a quaternary ammonium cation antimicrobial agent, is a potent hOCT2 inhibitor (IC_{50} = 88.16 ± 7.14 nM). Moreover, dequalinium inhibited hOCT2-mediated transport of platinum anti-cancer agents (cisplatin and oxaliplatin) in a concentration-dependent manner. Our study is the first to demonstrate the construction of a novel machine learning-based QSAR model for hOCT2 inhibitors and identify a novel hOCT2 inhibitor among FDA-approved drugs using this model.

Keywords Dequalinium, Drug repositioning, Machine learning, Organic cation transporter 2, Quantitative structure-activity relationship

Drug transporters, which have been identified and characterized in various human organs, are involved in drug disposition, response, and toxicity[1]. Organic cation transporter 2 (OCT2/*SLC22A2*) is a key transporter that facilitates the transport of various endogenous and exogenous organic cations[2,3]. As OCT2 transports platinum anti-cancer agents such as cisplatin and oxaliplatin into the kidney[4], inner ear cochlea[5], and dorsal root ganglion[6], OCT2 is closely related to the development of adverse effects of platinum anti-cancer agents.

The single-nucleotide polymorphism rs316019 in *hOCT2*, which adversely affects the function of hOCT2, is inversely correlated with cisplatin-induced nephrotoxicity/ototoxicity (CIN/CIO)[7]. In *Oct2* knockout mice, CIN/CIO[5] and oxaliplatin-induced peripheral neuropathy (OIPN)[8] were not observed. In addition, cimetidine, a typical OCT2 inhibitor, reduces CIN/CIO and OIPN in mice at concentrations much higher than the clinical dose[5]. Our previous studies demonstrated that proton pump inhibitors (PPIs) have off-target OCT2 inhibitory effects and that CIN/CIO and OIPN were suppressed by treatment with PPIs at a clinical dose[9–13]. Therefore, drugs that inhibit OCT2 may serve as prophylactic agents against CIN/CIO and OIPN.

The quantitative structure–activity relationship (QSAR) is a popular tool for identifying the relationship between chemical structure and biological activity[14]. Recently, novel QSAR applications have developed rapidly owing to the remarkable advancements in artificial intelligence techniques, including machine learning and the development of molecular databases[15]. In particular, machine learning techniques are attracting attention as promising tools for QSAR modeling[16], and machine learning-based QSAR models have been applied to drug repositioning, advancement of precision medicine, and drug discovery[17]. In the pharmacokinetic field, QSAR models of various drug transporters, including organic anion transporting polypeptide 1B1 (SLCO1B1), P-glycoprotein (ABCB1), and breast cancer resistance protein (ABCG2), have been developed[18–20]. The QSAR model of hOCT2 in flavonoids has been reported[21]. However, little information is available regarding the QSAR model of hOCT2 inhibitors in FDA-approved drugs.

[1]Department of Hospital Pharmacy, School of Pharmaceutical Sciences, Osaka University, Suita, Osaka 565-0871, Japan. [2]Department of Pharmacy, Osaka University Hospital, 2-15 Yamadaoka, Suita, Osaka 565-0871, Japan. ✉email: ikemurak@hp-drug.med.osaka-u.ac.jp

Parameters	Values
Accuracy	0.87
Precision	0.93
Recall	0.87
F1 score	0.89
Loss function	0.54

Table 1. The performance status of the QSAR model for hOCT2 inhibitors.

Classification by ATC code	Number of drugs
Antineoplastic and immunomodulating agents	29
Nervous system	17
Blood and blood forming organs	13
Alimentary tract and metabolism	12
Cardiovascular system	12
Antiinfectives for systemic use	11
Genito urinary system and sex hormones	9
Respiratory system	9
Dermatologicals	6
Musculo-skeletal system	6
Sensory organs	4
Systemic hormonal preparations, Excl. sex hormones and insulins	2
Antiparasitic products, insecticides and repellents	2
Various	7
Do not have ATC code	23

Table 2. Classification of the 162 drugs (predicted value ≥ 0.95) by ATC code.

In the present study, we explored novel hOCT2 inhibitors among FDA-approved drugs using a machine learning-based QSAR model.

Results

Establishment and evaluation of the QSAR model for hOCT2 inhibitors

Following the procedure described in the Materials and Methods section, we established a machine learning-based QSAR model for hOCT2 inhibitors based on the ChEMBL database. Our established model (Python files) is shown in Supplementary Information 1. The performance evaluation of the QSAR model for hOCT2 inhibitors is summarized in Table 1. If the accuracy, precision, recall, and F1 score of the QSAR model are close to 1, it means that the QSAR model is good. The loss function is a measure of how well a model predicts an expected outcome. A loss function close to 0 means a good QSAR model. As shown in Table 1, the accuracy, precision, recall, F1 score, and loss function of the proposed QSAR model were 0.87, 0.93, 0.87, 0.89, and 0.54, respectively. These results suggest that the QSAR model constructed in this study is highly predictive.

Screening of hOCT2 inhibitors from DrugBank database

We predicted the hOCT2 inhibitory activity of 11,281 compounds extracted from the DrugBank database using the QSAR model. The predicted values are listed in Supplementary Information 2. As shown in Supplementary Information 2, 1,232 compounds had a predicted value of ≥ 0.95. Among them, 162 were FDA-approved drugs. Table 2 shows the classification of the 162 compounds using Anatomical Therapeutic Chemical (ATC) code. Among the 162 compounds, drugs such as antineoplastic, antibacterial, antiviral, and antifungal agents, which are clinically unlikely to be used in combination with cisplatin, were excluded from the list of candidate hOCT2 inhibitors. Finally, we selected 15 compounds [hydroxocobalamin (predicted value: 0.999), methylcobalamin (0.999), cyanocobalamin (0.991), pemirolast (0.976), epinastine (0.971), riboflavin (0.969), famotidine (0.969), folic acid (0.965), FAD (0.961), rebamipide (0.960), tizanidine (0.960), dequalinium (0.955), flavoxate (0.953), ketotifen (0.952), and cromoglicate sodium (0.950)] as candidate hOCT2 inhibitors.

Validation on hOCT2 inhibitory effect of the candidate compounds

To assess whether the 15 candidate compounds inhibit hOCT2-mediated transport of ASP^+, the uptake of ASP^+ (5 μM) was measured in the absence or presence of cimetidine (a typical hOCT2 inhibitor, 1 mM) or the candidate compounds (1 and 10 μM). The hOCT2-mediated transport of ASP^+ was determined by subtracting the uptake in HEK vector cells from that in HEK-hOCT2 cells. Figure 1 shows the inhibitory effect of the 15 candidate compounds and cimetidine on hOCT2-mediated transport of ASP^+. First, we confirmed the functionality of HEK293 cells expressing hOCT2 using cimetidine (an OCT2 inhibitor). As shown in Fig. 1, the

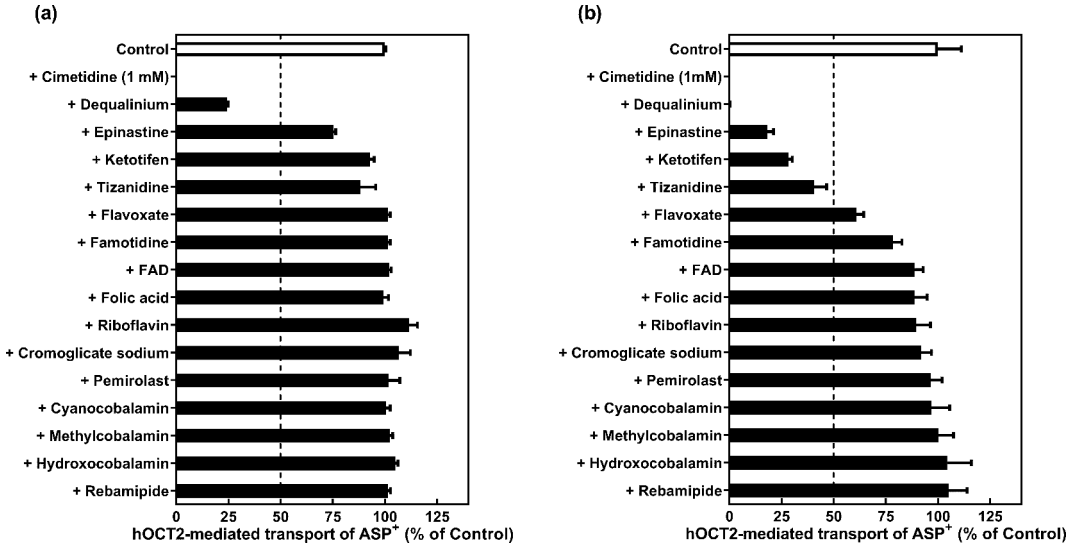

Fig. 1. Inhibition of candidate compounds against hOCT2-mediated transport of ASP^+. HEK-hOCT2 or HEK-vector cells were incubated at 37°C for 5 min with ASP^+ (5 μM, pH 7.4) in the absence or presence of cimetidine (a typical OCT2 inhibitor, 1 mM) or candidate compounds at a concentration of 1 μM (**a**) and 10 μM (**b**). The hOCT2-mediated transport of ASP^+ was determined by subtracting the uptake in HEK-vector cells from that in HEK-hOCT2 cells. The hOCT2-mediated transport of ASP^+ after treatment of control (vehicle) was set at 100%. Each column represents the mean ± S.E. of three independent experiments using three monolayers.

hOCT2-mediated transport of ASP^+ was potently inhibited by cimetidine (1 mM). This finding indicates the activity and specificity of hOCT2 in HEK-hOCT2 cells. Next, we examined the inhibitory effect of 15 candidate compounds (1 and 10 μM) for hOCT2-mediated transport of ASP^+. At a concentration of 1 μM (Fig. 1a), the inhibitory effect of 14 compounds excluding dequalinium for hOCT2 was not observed. At a concentration of 10 μM (Fig. 1b), high inhibitory activities (≥ 50%) for hOCT2 were observed in 4 compounds (dequalinium, epinastine, ketotifen, and tizanidine). In addition, the apparent IC_{50} values of dequalinium, which had the most potent inhibitory effect on hOCT2, were calculated from the inhibition plots (Fig. 2). The apparent IC_{50} of dequalinium against ASP^+ transport *via* hOCT2 was 88.16 ± 7.14 nM.

Inhibitory effect of dequalinium for hOCT2-mediated transport of cisplatin and oxaliplatin

To assess whether dequalinium inhibits hOCT2-mediated transport of cisplatin and oxaliplatin, the uptake of cisplatin and oxaliplatin (10 μM) was measured for 15 min in the absence or presence of various concentrations of dequalinium in HEK-vector and HEK-hOCT2 cells (Fig. 3a, b). Dequalinium inhibited the hOCT2-mediated transport of cisplatin and oxaliplatin in a concentration-dependent manner. The apparent IC_{50} of dequalinium against transport of cisplatin and oxaliplatin *via* hOCT2 was 18.81 ± 9.93 nM and 11.37 ± 5.32 nM, respectively.

Discussion

To date, no QSAR model for hOCT2 inhibitors has been established. To the best of our knowledge, this is the first study in which a machine learning-based QSAR model for hOCT2 inhibitors was constructed. In addition, we found that dequalinium is a potent hOCT2 inhibitor among the FDA-approved drugs using the machine learning-based QSAR model.

A previous study explored hOCT2 inhibitors among a library of 910 prescription drugs and drug-like compounds[22]. In general, screening through high-throughput assays requires significant capital investment and the preparation of extensive compound libraries, which are costly and time-consuming. Furthermore, the number of compounds that can be screened heavily depends on library size and is consequently limited for analysis. In contrast, using an available dataset of compounds with known biological activities and calculating their molecular descriptors, a QSAR model can be constructed using standard statistical methods. By applying a QSAR model to a large-scale dataset, as demonstrated in this study, novel compounds were identified. Therefore, screening using QSAR models is a powerful tool in drug discovery research. Kido et al.[22] identified six compounds (disopyramide, dipyridamole, imipramine, tacrine, orphenadrine, and ondansetron) as clinical hOCT2 inhibitors among 910 compounds. As shown in Supplementary Information 2, our QSAR model recognized these compounds as hOCT2 inhibitors. These findings suggest that the QSAR model constructed in this study is highly valid.

Dequalinium is a quaternary ammonium cation antimicrobial agent used to treat common infections of the mouth and throat, as well as vaginal candidiasis[23]. Dequalinium targets various proteins and has antibacterial, antiviral, antifungal, antiparasitic, and anticancer properties[23]. However, the inhibitory effect of dequalinium on hOCT2 remains unclear. As shown in Fig. 2, the apparent IC_{50} value of dequalinium against ASP^+ transport

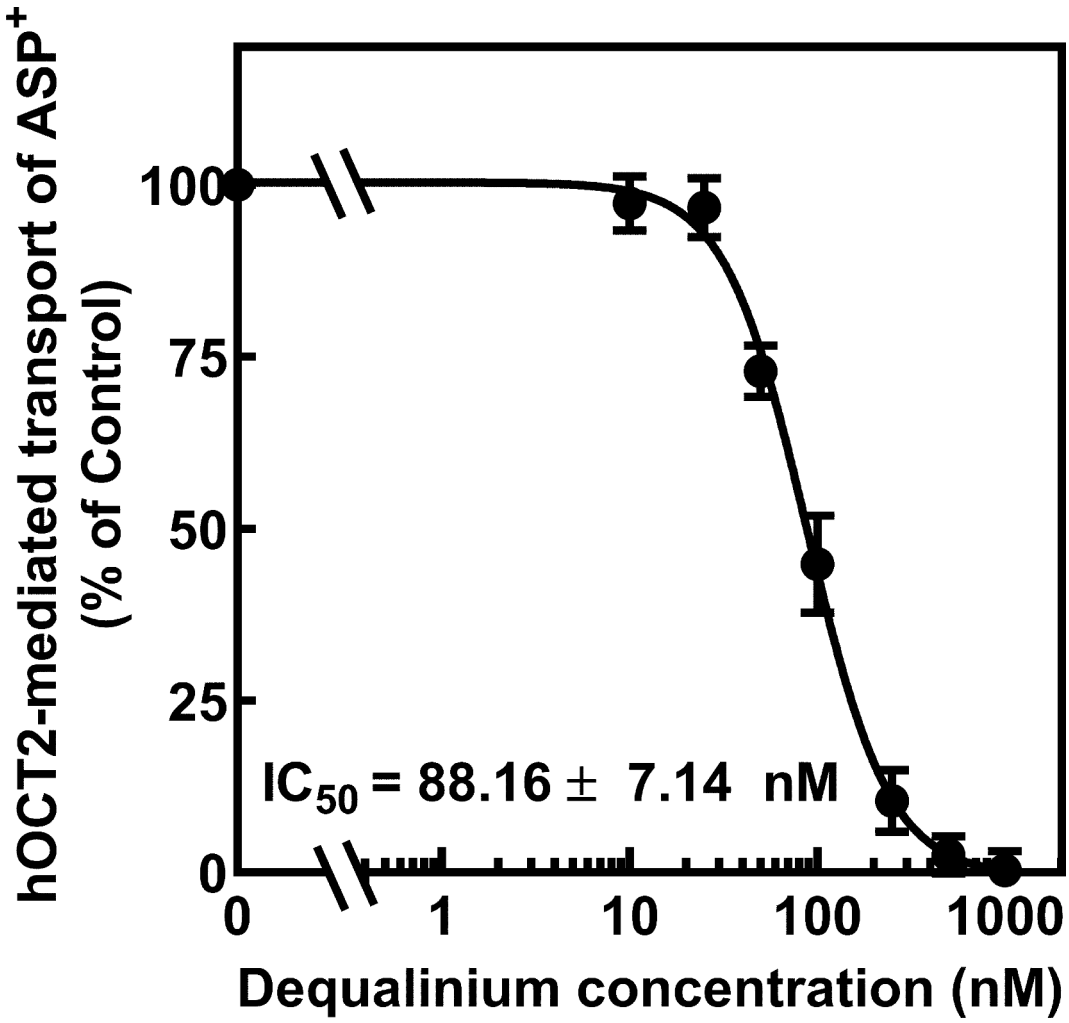

Fig. 2. Inhibition of dequalinium against hOCT2-mediated transport of ASP^+. HEK-hOCT2 or HEK-vector cells were incubated at 37 °C for 5 min with ASP^+ (5 μM, pH 7.4) in the presence of various concentrations of dequalinium. The hOCT2-mediated transport of ASP^+ was determined by subtracting the uptake in HEK vector cells from that in HEK-hOCT2 cells. Each point represents the mean ± S.E. of three independent experiments using three monolayers. When the standard errors of the means were small, they were contained within the symbols. The apparent IC_{50} values were calculated by fitting the data to a sigmoidal dose-response regression curve.

via hOCT2 was 88.16 ± 7.14 nM. Because the apparent IC_{50} value of cimetidine, a typical OCT2 inhibitor, was reported to be approximately 26 μM[24], we assumed that dequalinium has a considerable potent inhibitory effect against hOCT2. Interestingly, dequalinium potently inhibited the hOCT2-mediated transport of platinum anti-cancer agents (cisplatin and oxaliplatin) (Fig. 3), indicating that dequalinium could modulate the hOCT2-mediated disposition of cisplatin and oxaliplatin. While dequalinium is generally well tolerated and considered safe at therapeutic doses, it exhibits neurotoxicity with an IC_{50} value of 0.46 μM in cultured cerebellar granule neurons[25]. Furthermore, high doses of dequalinium caused drug-induced hepatic and renal injuries in mice[26]. Thus, dequalinium is likely safe when administered at low concentrations that inhibit hOCT2 without inducing toxicity. In contrast, we could not assess whether dequalinium exhibited an inhibitory effect on hOCT2 at clinical concentrations because no information is available regarding the pharmacokinetics and/or the plasma concentration of dequalinium in humans. Further studies are required to assess the prophylactic effects of dequalinium on CIN/CIO and OIPN.

In addition to dequalinium, the 50% inhibitory effects for hOCT2 were observed in three compounds, epinastine, ketotifen, and tizanidine, at a concentration of 10 μM (Fig. 1b). When we conducted the inhibition study of the 15 candidate compounds at a concentration of 1 μM, the inhibitory effect of 14 compounds excluding dequalinium for hOCT2 was not observed (Fig. 1a). Because the maximum unbound plasma concentrations of epinastine, ketotifen, and tizanidine were estimated to be less than 1 μM, it is unlikely that these 3 compounds inhibit hOCT2 activity at clinical concentrations. In addition, the 11 other compounds excluding dequalinium, epinastine, ketotifen, and tizanidine did not exhibit any inhibitory effect against hOCT2 at a concentration of 10 μM (Fig. 1b). In the present study, the compounds with an inhibition constant of ≤ 100 μM for hOCT2 were

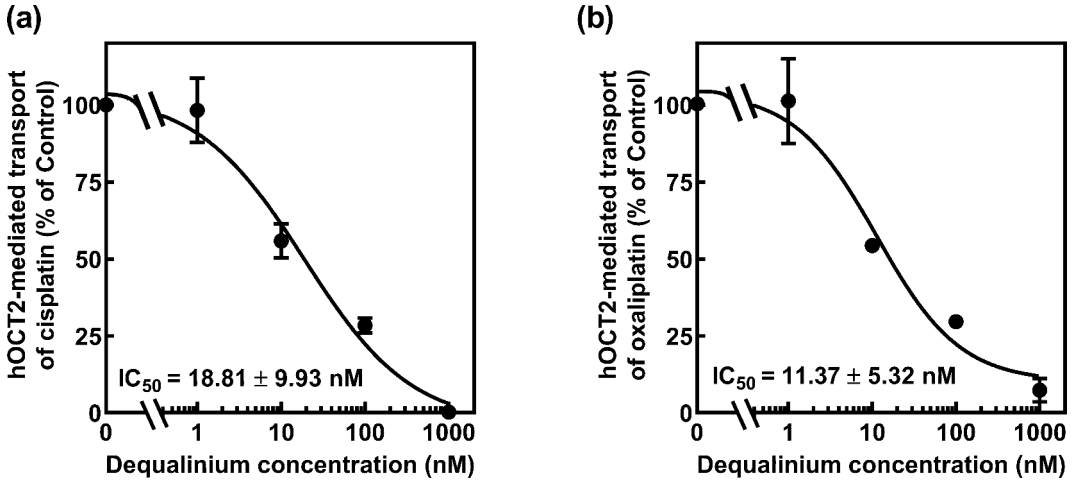

Fig. 3. Inhibition of dequalinium against hOCT2-mediated transport of cisplatin (**a**) and oxaliplatin (**b**). HEK-hOCT2 or HEK-vector cells were incubated at 37°C for 15 min with cisplatin or oxaliplatin (10 μM, pH 7.4) in the presence of various concentrations of dequalinium. Each point represents the mean ± S.E. of three independent experiments using three monolayers. When the standard errors of the means were small, they were contained within the symbols. The apparent IC_{50} values were calculated by fitting the data to a sigmoidal dose-response regression curve.

defined as compounds with an inhibitory effect against hOCT2 in the training data of our QSAR models. It is conceivable that the inhibitory effect on hOCT2 may have been validated using these compounds at higher concentrations. However, we did not conduct the experiments at concentrations exceeding the clinical level because our aim was to identify clinically applicable compounds.

In contrast, among the 15 tested candidate compounds, the IC_{50} values of famotidine (36.1 μM) and epinastine (4.3 μM) were registered in the ChEMBL database and included in the training data of our QSAR model. As shown in Fig. 1b, the 50% inhibitory effects for hOCT2 were observed in epinastine but not famotidine at a concentration of 10 μM. Thus, these findings suggest that our QSAR model has high prediction accuracy. However, our QSAR model was limited. Our QSAR could not predict the hOCT2 inhibitory activity of compounds whose Morgan fingerprints could not be calculated from the DrugBank database. Because various methods can be employed for calculating Morgan fingerprints, molecular descriptors, and machine learning, it is possible to construct better QSAR models by combining these methods.

Several OCT2 inhibitors simultaneously inhibit multidrug and toxin extrusion 1 (MATE1/*SLC47A1*) and MATE2-K/*SLC47A2*[27] whereas tubular secretion of cisplatin was mediated mainly by hMATE1 and slightly by hMATE2-K[28,29]. Since hMATE2-K is specifically expressed in the kidney[30], it plays a minimal role in the development of OIPN. Therefore, we focused on hMATE1 activity and assessed the inhibitory effects of dequalinium (100 nM) on ASP^+ transport in HEK-hMATE1 cells. As shown in Supplementary Fig. 1, no inhibitory effect of dequalinium on hMATE1 was observed. When we conducted the uptake study of dequalinium in HEK-hOCT2 and HEK-vector cells, no significant differences were observed in uptake of dequalinium between the two cell lines (Supplementary Fig. 2). As dequalinium is not transported into the cells *via* hOCT2, it may not be concentrated in the cells. It is likely that dequalinium has little inhibitory effect on hMATE1 activity. Moreover, the inhibitory effect of dequalinium (100 nM) on the hOCT1-mediated transport of ASP was not observed. (Supplementary Fig. 3). Thus, these findings suggested that dequalinium specifically inhibits hOCT2 activity.

In conclusion, our study is the first to construct a novel machine learning-based QSAR model for hOCT2 inhibitors. We identified a novel hOCT2 inhibitor among FDA-approved drugs using this model. Thus, screening using machine learning-based QSAR models can serve as a powerful tool in drug repositioning research.

Materials and methods

Materials

The following compounds were purchased commercially from the following sources: 4-(4-(dimethylamino) styryl)-*N*-methylpyridinium iodide (ASP^+, Oakwood Chemical, Inc, SC, USA), epinastine hydrochloride, flavoxate hydrochloride, ketotifen fumarate, pemirolast potassium, tizanidine hydrochloride, riboflavin (Tokyo Chemical Industry, Tokyo, Japan), cimetidine, cisplatin, cyanocobalamin, flavin adenine dinucleotide disodium salt n-hydrate (FAD), folic acid, hydroxocobalamin acetate, methylcobalamin, sodium cromoglicate (FUJIFILM Wako Pure Chemical, Osaka, Japan), famotidine (Sigma Chemical Co. St. Louis, MO, USA), oxaliplatin (LC Laboratories, Woburn, MA, USA), and dequalinium chloride (Cayman Chemical Company, MI, USA). All other chemicals used were of the highest available purity.

Quantitative structure-activity relationship (QSAR) modeling and screening

Dataset acquisition and curation

We identified 74 compounds with IC_{50} and Ki values against hOCT2 (ChEMBL ID: CHEMBL1743122) from the ChEMBL database (https://www.ebi.ac.uk/chembl/). For the compounds with multiple IC_{50} or Ki values, the average value was used as the inhibition constant. The information of 74 compounds are listed in Supplementary Information 3. Based on the ASCII-encoded SMILES representing the molecular structure, the Morgan fingerprint (2048-bit, radius = 3) and molecular descriptors were calculated using RDkit (https://github.com/rdkit/rdkit/releases/tag/Release_2016_09_4) and Mordred software[31], respectively. Compounds with an inhibition constant of ≤ 100 μM were defined as compounds with an inhibitory effect against hOCT2. Features within the Morgan fingerprints that exhibited a low correlation with the inhibitory effect on hOCT2 were excluded using a filtering method. Next, the Morgan fingerprint and molecular descriptors were calculated for 11,281 compounds registered in the DrugBank database[32] using the method described above. If the features of the molecular descriptors could not be calculated for the compounds in both the ChEMBL and DrugBank databases, these features were not utilized for the analysis. Each feature was standardized as an average of 0 and a standard deviation of 1.

Development of QSAR model for hOCT2 inhibitors and screening of hOCT2 inhibitors from the DrugBank database

The Morgan fingerprints, molecular descriptors, and presence or absence of hOCT2 inhibition of the 74 compounds extracted from ChEMBL were utilized as training data, and the Morgan fingerprints and molecular descriptors of the 11,281 compounds extracted from DrugBank served as prediction data. A QSAR model for hOCT2 inhibitors was constructed using Keras (https://keras.io/), which is one of the neural network libraries. The hyperparameters of the neural network were estimated using Optuna (https://github.com/pfnet/optuna). After oversampling the training data using ADASYN[33], the best parameters were determined by 5-fold cross-validation, which were utilized for the final model. The model was evaluated using the following parameters: accuracy, precision, recall, F1 score, and loss function. The accuracy, precision, recall, and F1 score were calculated using the following formulas. Loss function was calculated using model.evaluate(), which is a Keras module. Python™ (Jupyter Notebook) was used to construct the QSAR model and calculate the predicted values for the compounds in DrugBank.

$$Accuracy = (TP + TN)/(TP + TN + FP + FN)$$

$$Precision = TP/(TP + FP)$$

$$Recall = TP/(TP + FN)$$

$$F1\ score = (2Precision \times Recall)/(Precision + Recall)$$

$$TP\text{: }True\ Positive,\ TN\text{: }True\ Negative,\ FP\text{: }False\ Positive,\ FN\text{: }False\ Negative$$

Cell culture

The human embryonic kidney cell line HEK293 (American Type Culture Collection, CRL-1573) stably expressing hOCT1, hOCT2, hMATE1, or mock transfectants was kindly provided by Dr. Atsushi Yonezawa (Department of Pharmacy, Kyoto University Hospital, Japan) and cultured as described previously[34]. The HEK-hOCT2 and HEK-vector cells were used between passages 82 and 90. Cells were maintained at 37 °C in a humidified 5% CO_2 atmosphere.

Validation on hOCT2 inhibitory effect of candidate compounds

HEK-hOCT2 and HEK-vector cells (1.0×10^6 cells/dish) were seeded in 3.5-cm dishes with Dulbecco's modified Eagle's medium (WAKO Pure Chemical) supplemented with 10% fetal bovine serum. Cell monolayers formed after 48 h of culture were used for the uptake studies. Cellular uptake of ASP^+, which is a well-established substrate of OCT2[22], was determined using monolayer cultures of HEK-hOCT2 and HEK-vector cells at 37 °C. The incubation medium was 145 mM NaCl, 3 mM KCl, 1 mM $CaCl_2$, 0.5 mM $MgCl_2$, 5 mM D-glucose, and 5 mM HEPES (pH 7.4). HEK-hOCT2 and HEK-vector cells were incubated for 5 min with 5 μM ASP^+ in the absence or presence of cimetidine (a typical OCT2 inhibitor, 1 mM) and the candidate compounds (1 and 10 μM). Furthermore, an inhibition experiment was conducted in the absence or presence of the candidate compound with the greatest inhibitory effect, and the apparent IC_{50} values were generated from curve fits using GraphPad Prism version 8.4.3 (GraphPad Software Inc., San Diego, CA, USA). The apparent IC_{50} values were calculated from the inhibition plots according to the equation : $V = V_{bottom} + (V_{top} - V_{bottom})/[1 + (\log I/IC_{50})^n]$ by nonlinear least square regression analysis, where V is the transport velocity, V_{bottom} is the transport velocity at the highest concentration of inhibitor, V_{top} is the transport velocity without inhibitor, $I$is the concentration of the inhibitor, and n is the Hill coefficient. To evaluate the accumulation of ASP^+ in the cells, the cells were solubilized in 5% sodium dodecyl sulfate solution and the fluorescence of ASP^+ was measured using a fluorescence spectrophotometer (SH-9000lab, CORONA, Ibaraki, Japan) at 485 nm excitation/607 nm emission. The protein contents of the solubilized cells were measured using a BCA protein assay kit (Thermo Fisher Scientific, Waltham, MA, USA) with bovine serum albumin as a standard. The hOCT2-mediated transport of ASP^+ was determined by subtracting the uptake in HEK-vector cells from that in HEK-hOCT2 cells.

Inhibitory effect of dequalinium for hOCT2-mediated transport of cisplatin and oxaliplatin

Cisplatin and oxaliplatin uptake studies were conducted according to the method described for ASP^+. The cells were incubated with 10 μM cisplatin and oxaliplatin for 15 min in the presence or absence of 100 nM dequalinium. After the inhibition experiments, the cellular pellet was suspended in 1 mL of ultrapure water to obtain a homogeneous cell suspension. The aliquots were solubilized in 0.5 N NaOH. The remaining cell

suspension was mineralized with 70% HNO_3 and then completely dried at 100℃. The platinum content was determined by inductively coupled plasma mass spectrometry using an Agilent7700 series (Agilent Technologies, Santa Clara, CA, USA). The instrument settings were optimized to obtain the maximum sensitivity of platinum. Dry platinum-containing material was dissolved in 1 mL of 5% HNO_3 with 0.1 ng/mL thallium, which was used as an internal standard. The most abundant platinum and thallium isotopes were observed at m/z 195 and 205, respectively.

Statistical analyses

The experimental data are expressed as the mean ± standard error (S.E.). Statistical comparisons between the two groups were performed using an unpaired *t*-test in GraphPad Prism version 8.4.3. Differences were considered statistically significant at $p < 0.05$.

Data availability

All data generated or analyzed during this study are included in this published article and its Supplementary Information files.

Received: 7 August 2024; Accepted: 8 November 2024
Published online: 20 January 2025

References

1. Ikemura, K., Iwamoto, T. & Okuda, M. Altered functions and expressions of drug transporters in liver, kidney and intestine in disorders of local and remote organs: possible role of oxidative stress in the pathogenesis. *Expert Opin. Drug Metab. Toxicol.* **5**, 907–920 (2009).
2. Okuda, M., Urakami, Y., Saito, H. & Inui, K. Molecular mechanisms of organic cation transport in OCT2-expressing Xenopus oocytes. *Biochim. Biophys. Acta*. **1417**, 224–231 (1999).
3. Urakami, Y. et al. Distinct characteristics of organic cation transporters, OCT1 and OCT2, in the basolateral membrane of renal tubules. *Pharm. Res.* **18**, 1528–1534 (2001).
4. Yonezawa, A. & Inui, K. Organic cation transporter OCT/SLC22A and H(+)/organic cation antiporter MATE/SLC47A are key molecules for nephrotoxicity of platinum agents. *Biochem. Pharmacol.* **81**, 563–568 (2011).
5. Ciarimboli, G. et al. Organic cation transporter 2 mediates cisplatin-induced oto- and nephrotoxicity and is a target for protective interventions. *Am. J. Pathol.* **176**, 1169–1180 (2010).
6. Sprowl, J. A. et al. Oxaliplatin-induced neurotoxicity is dependent on the organic cation transporter OCT2. *Proc. Natl. Acad. Sci. U. S. A.* 110, 11199–11204 (2013).
7. Iwata, K. et al. Effects of genetic variants in SLC22A2 organic cation transporter 2 and SLC47A1 multidrug and toxin extrusion 1 transporter on cisplatin-induced adverse events. *Clin. Exp. Nephrol.* **16**, 843–851 (2012).
8. Huang, K. M. et al. Neuronal uptake transporters contribute to oxaliplatin neurotoxicity in mice. *J. Clin. Invest.* **130**, 4601–4606 (2020).
9. Hiramatsu, S. I., Ikemura, K., Fujisawa, Y., Iwamoto, T. & Okuda, M. Concomitant lansoprazole ameliorates cisplatin-induced nephrotoxicity by inhibiting renal organic cation transporter 2 in rats. *Biopharm. Drug Dispos.* **41**, 239–247 (2020).
10. Ikemura, K., Hiramatsu, S. & Okuda, M. Drug repositioning of proton pump inhibitors for enhanced efficacy and safety of cancer chemotherapy. *Front. Pharmacol.* **8**, 911 (2017).
11. Ikemura, K. et al. Co-administration of proton pump inhibitors ameliorates nephrotoxicity in patients receiving chemotherapy with cisplatin and fluorouracil: a retrospective cohort study. *Cancer Chemother. Pharmacol.* **79**, 943–949 (2017).
12. Kobayashi, A., Ikemura, K., Wakai, E., Kondo, M. & Okuda, M. Proton pump inhibitors ameliorate oxaliplatin-induced peripheral neuropathy: retrospective analysis of two real-world clinical databases. *Anticancer Res.* **43**, 5613–5620 (2023).
13. Wakai, E. et al. Repositioning of lansoprazole as a protective agent against cisplatin-induced ototoxicity. *Front. Pharmacol.* **13**, 896760 (2022).
14. Cherkasov, A. et al. QSAR modeling: where have you been? Where are you going to? *J. Med. Chem.* **57**, 4977–5010 (2014).
15. Lo, Y. C., Rensi, S. E., Torng, W. & Altman, R. B. Machine learning in chemoinformatics and drug discovery. *Drug Discov Today*. **23**, 1538–1546 (2018).
16. Keyvanpour, M. R. & Shirzad, M. B. An analysis of QSAR research based on machine learning concepts. *Curr. Drug Discov Technol.* **18**, 17–30 (2021).
17. Tropsha, A., Isayev, O., Varnek, A., Schneider, G. & Cherkasov, A. Integrating QSAR modelling and deep learning in drug discovery: the emergence of deep QSAR. *Nat. Rev. Drug Discov* (2023).
18. Ahmad, S., Gupta, D., Ahmed, T. & Islam, A. Designing of new tetrahydro-beta-carboline-based ABCG2 inhibitors using 3D-QSAR, molecular docking, and DFT tools. *J. Biomol. Struct. Dyn.* **41**, 14016–14027 (2023).
19. Gui, C., Li, Y. & Peng, T. Development of predictive QSAR models for the substrates/inhibitors of OATP1B1 by deep neural networks. *Toxicol. Lett.* **376**, 20–25 (2023).
20. Mora Lagares, L. & Novic, M. Recent advances on P-glycoprotein (ABCB1) transporter modelling with in silico methods. *Int. J. Mol. Sci.* **23** (2022).
21. Bi, Y. et al. 3D-QSAR analysis of the interactions of flavonoids with human organic cation transporter 2. *Toxicol. Lett.* **368**, 1–8 (2022).
22. Kido, Y., Matsson, P. & Giacomini, K. M. Profiling of a prescription drug library for potential renal drug-drug interactions mediated by the organic cation transporter 2. *J. Med. Chem.* **54**, 4548–4558 (2011).
23. Bailly, C. Medicinal applications and molecular targets of dequalinium chloride. *Biochem. Pharmacol.* **186**, 114467 (2021).
24. Biermann, J. et al. Characterization of regulatory mechanisms and states of human organic cation transporter 2. *Am. J. Physiol. Cell. Physiol.* **290**, C1521–1531 (2006).
25. Chan, C. F. & Lin-Shiau, S. Y. Suramin prevents cerebellar granule cell-death induced by dequalinium. *Neurochem Int.* **38**, 135–143 (2001).
26. Gamboa-Vujicic, G., Emma, D. A., Liao, S. Y., Fuchtner, C. & Manetta, A. Toxicity of the mitochondrial poison dequalinium chloride in a murine model system. *J. Pharm. Sci.* **82**, 231–235 (1993).
27. Tsuda, M. et al. Involvement of human multidrug and toxin extrusion 1 in the drug interaction between cimetidine and metformin in renal epithelial cells. *J. Pharmacol. Exp. Ther.* **329**, 185–191 (2009).
28. Yokoo, S. et al. Differential contribution of organic cation transporters, OCT2 and MATE1, in platinum agent-induced nephrotoxicity. *Biochem. Pharmacol.* **74**, 477–487 (2007).

29. Yonezawa, A., Masuda, S., Yokoo, S., Katsura, T. & Inui, K. Cisplatin and oxaliplatin, but not carboplatin and nedaplatin, are substrates for human organic cation transporters (SLC22A1-3 and multidrug and toxin extrusion family). *J. Pharmacol. Exp. Ther.* **319**, 879–886 (2006).
30. Masuda, S. et al. Identification and functional characterization of a new human kidney-specific H+/organic cation antiporter, kidney-specific multidrug and toxin extrusion 2. *J. Am. Soc. Nephrol.* **17**, 2127–2135 (2006).
31. Moriwaki, H., Tian, Y. S., Kawashita, N. & Takagi, T. Mordred: a molecular descriptor calculator. *J. Cheminform.* **10**, 4 (2018).
32. Wishart, D. S. et al. DrugBank 5.0: a major update to the DrugBank database for 2018. *Nucleic Acids Res.* **46**, D1074–D1082 (2018).
33. He, H. B., Bai, Y., Garcia, E. A. & Li, S. T. ADASYN: Adaptive Synthetic Sampling Approach for Imbalanced Learning. *Ieee International Joint Conference on Neural Networks, Vols 1–8*, 1322–1328 (2008). (2008).
34. Sato, T. et al. Transcellular transport of organic cations in double-transfected MDCK cells expressing human organic cation transporters hOCT1/hMATE1 and hOCT2/hMATE1. *Biochem. Pharmacol.* **76**, 894–903 (2008).

Acknowledgements

We would like to thank Editage (www.editage.jp) for the English language editing.

Author contributions

K.I. and M.O. contributed to study conception and design. F.Y. was involved in establishing and screening machine learning-based QSAR models. F.Y., K.I., K.M., and M.U. performed in vitro experiments. F.Y. and K. I. analyzed and interpreted the data and drafted the manuscript. K. I. and M. O. critically revised the manuscript. All the authors have read and approved the final version of the manuscript.

Declarations

Competing interests

The authors declare no competing interests.

Additional information

Supplementary Information The online version contains supplementary material available at https://doi.org/10.1038/s41598-024-79377-0.

Correspondence and requests for materials should be addressed to K.I.

Reprints and permissions information is available at www.nature.com/reprints.

Publisher's note Springer Nature remains neutral with regard to jurisdictional claims in published maps and institutional affiliations.